A biodegradable, biocompatible transdermal device derived from carboxymethyl cellulose and multi-walled carbon nanotubes for sustained release of diclofenac sodium†

Barun Mandal,[a] Dipankar Das,[a] Arun Prabhu Rameshbabu,[b] Santanu Dhara[b] and Sagar Pal*[a]

A hybrid nanocomposite hydrogel (CMC–MWCNT) has been fabricated using carboxymethyl cellulose (CMC) and acid-functionalized multi-walled carbon nanotubes (MWCNTs) at room temperature for transdermal delivery of diclofenac sodium. With variation of MWCNT concentration, various grades of nanocomposites have been prepared and an optimized composite (CMC–MWCNT 3) has been considered with lower % swelling and higher gel strength. The synthesized nanocomposite has been characterized using FTIR spectroscopy, FESEM, TGA, AFM and TEM analyses. The gel strength of the nanocomposites has been measured by determining the rheological parameters. The biodegradability of the composite material has been confirmed using lysozyme hydrochloride. A biocompatibility study using primary rat fibroblasts (RFBs) confirmed the non-cytotoxic nature of the composite. The release profiles of diclofenac sodium indicate that the synthesized composite releases the drug in a sustained manner and would be a better alternative for transdermal devices.

1. Introduction

In the last few decades, biopolymeric hydrogels have received a great deal of attention in various applications such as waste-water treatment,[1] adsorption,[2] tissue engineering[3,4] and drug delivery.[5–7] Hydrogels are three-dimensional, soft cross-linked polymeric networks that are able to absorb large quantities of water.[8,9] However, the applications of mechanically weak and brittle hydrogels are limited where high mechanical properties are concerned.[10] Recently, hybrid nanocomposite hydrogels have opened a new avenue and are able to improve the mechanical strength of hydrogels. In principle, the nano-composite hydrogels are prepared by incorporation of nano-fillers onto the hydrogel matrix.[11] The stability of these composites depends on the electrostatic force of attraction, hydrogen bonding, and van der Wall's forces between the hydrogel and the nanofiller.[12–15] Owing to the high specific surface area, resembling with human tissues, ability to water absorption and stimuli responsiveness, hybrid nanocomposite hydrogels are widely used in various fields such as adsorption,[16]

drug delivery,[17,18] photo-degradation[19] and so on. Although various hybrid nanocomposites are used as drugs carrier for oral delivery but the application of nanocomposites in trans-dermal drug delivery are less studied.

Our interest is lying on the development of carboxymethyl cellulose (CMC) based biocompatible, biodegradable hybrid nanocomposite for transdermal drug delivery. Transdermal delivery system is an innovative drug delivery system to accomplish a systemic effect through skin application.[20,21] The drug molecules reside in the drug-in adhesive materials, released through the adhesive layer which remained in contact with the skin.[22] This method is commonly used owing to their ease and comfortable usage.[23] Besides, among various modes of drug delivery, transdermal system has several advantages which include the ability to attain steady-state drug concentration, avoid hepatic first-pass metabolism, enhanced patient adher-ence and reduced gastrointestinal adverse effects.[24]

Carboxymethyl cellulose (CMC) is a water-soluble anionic polysaccharide.[25,26] Because of its biocompatibility and biode-gradability, it is often used in the biomedical field,[27] lithium-ion battery,[28,29] super capacitors,[30] and biosensors.[31] On the other hand, carbon nanotubes (CNTs) demonstrate very interesting properties because of sp^2 hybridization of carbon–carbon bonds, and the resultant cylindrical arrangement of the gra-phene sheets.[32] It is also inexpensive, have rapid electron transfer kinetics, large surface area, and high electro-catalytic activity. The functionalized MWCNT and its composite have

[a]*Polymer Chemistry Laboratory, Department of Applied Chemistry, Indian School of Mines, Dhanbad-826004, India. E-mail: sagarpal1@hotmail.com*

[b]*Biomaterials and Tissue Engineering Laboratory, School of Medical Science & Technology, Indian Institute of Technology, Kharagpur-721302, India*

† Electronic supplementary information (ESI) available: Details of various characterizations, experimental techniques, and drug stability study. See DOI: 10.1039/c6ra00260a

also been employed in solar cell,[33] fuel cells,[34] biosensors,[35] tissue engineering applications.[36] Besides, diclofenac sodium is an anti-inflammatory drug (NSAID), used for the treatment of osteoarthritis, superficial, rheumatic diseases, minor and medium pain.[37,38] Although there are several reports on the development of transdermal devices for release of various drugs, still it is imperative to develop transdermal drug carriers through improving the drawbacks of the reported systems, such as inexpensiveness, biodegradability, biocompatibility, high loading efficiency and most importantly sustained release characteristics with excellent stability of the drug in the device, which are addressed herein.

Here, we have developed carboxymethyl cellulose (CMC) and acid functionalized multiwalled carbon nanotube (MWCNT) based hybrid nanocomposite hydrogel by ultrasonication at room temperature. The nanocomposite is biodegradable and non-cytotoxic towards rat fibroblasts (RFBs). It has sufficient gel strength for intended application of transdermal patch. The entrapment efficiency and loading efficiency of the optimized composite (CMC–MWCNT 3) are 90% and 15%, respectively. Moreover, the fabricated nanocomposite released the drug (diclofenac sodium) in a sustained way through permeable membrane in transdermal set up. The stability study predicts that ~98% drug molecules remained stable in the composite system, while the CMC demonstrates poor efficacy towards the drug stability. This is probably the first report on CMC–MWCNT based nanocomposite for sustained release of diclofenac sodium and undoubtedly be a good substitute of transdermal device for diclofenac sodium delivery.

2. Experimental

2.1 Materials

Carboxymethyl cellulose (CMC) (with DS-0.6) was received from Hindustan Gum and Chemicals Ltd., Haryana, India. Carboxylic acid functionalized (>8 wt%) MWCNT, with avg. diameter × L 9.5 nm × 1.5 μm was purchased from Sigma-Aldrich, USA. Cellulose acetate membrane was purchased from Himedia, India. Double distilled (Milli-Q) water was used for experimental works.

2.2 Preparation of CMC–MWCNT nanocomposite

Different amount (0.25, 0.5, 1 and 1.5 w/v%) of functionalized MWCNT were dispersed in aqueous solution in a beaker at room temperature (25 °C). After that, required quantity of CMC was added slowly to solution and stirred for 2 h. Subsequently, the resultant mixture was ultrasonicated for 2 h so that nanotubes were homogenously incorporated on the hydrogel network and formed hybrid nanocomposite hydrogel (CMC–MWCNT). The prepared nanocomposite hydrogels were dried on vacuum oven at 40 °C for 48 h.

2.3 Characterization

FTIR, TGA, FESEM, AFM and TEM analyses were performed to characterize the developed nanocomposite hydrogels. The experimental techniques and the instrument details are given in ESI.†

2.4 Swelling study and its kinetics

The stimuli-responsive behavior of CMC and CMC–MWCNT nanocomposite hydrogels were studied by evaluating the equilibrium swelling in a phosphate buffer (pH-7.4) at 32 °C. The detailed methodology is explained in ESI.†

Moreover, swelling rate was measured using Voigt model (eqn (1))[39]

$$S_t = S_e(1 - e^{-t/\tau}) \tag{1}$$

where S_t, S_e, t and τ are the swelling at time t, swelling at equilibrium, time and rate parameter, respectively.

2.5 Rheological experiments

The rheological properties of CMC and CMC–MWCNT composites were executed in swollen state at pH 7.4 using a rheometer (Bohlin Gemini-2, Malvern, United Kingdom). The frequency sweep experiments of nanocomposites were performed in the range of 1–10 Hz with a constant stress of 2 Pa at 37 °C. To measure the gel strength of the composites, oscillatory sweep measurements were carried out with constant frequency of 0.1 Hz and in different shear stress in the range of 0.1–200 Pa using parallel plate geometry. The tool gap was 500 μm. The shear viscosity of CMC and CMC–MWCNT nanocomposites were estimated in the shear rate range of 1 to 1000 s^{-1} at 37 °C.

2.6 Biodegradation study

Enzymatic degradation study of CMC–MWCNT 3 composite was executed using lysozyme hydrochloride solution in the same procedure as explained in the preceding literature.[40,41] The experimental procedure has been illustrated in ESI.†

2.7 Cytotoxicity test and morphological assessment

Cytotoxicity of the CMC–MWCNT 3 nanocomposite dissolved in DMEM high glucose medium containing 10% fetal calf serum, 100 U mL^{-1} penicillin and 100 μg mL^{-1} streptomycin (all purchased from Gibco, USA) was tested by cultivation of primary rat fibroblasts (RFBs). The media containing 1 mg mL^{-1} of nanocomposite was filtered with 0.22 μm syringe filters (Merck Millipore) before treating to the cells. The experimental procedure for the cytotoxicity study and morphological assessment is illustrated in ESI.†

2.8 *In vitro* drug delivery study

2.8.1 Determination of drug loading and entrapment efficiency. Diclofenac sodium (0.8 mg mL^{-1}) solution was mixed with CMC–MWCNT 3 nanocomposite suspension (7.5 mg mL^{-1}), stirred for 4 h, followed by centrifugation at 5000 rpm for 15 min, for precipitation of drug loaded composite. The process was repeated thrice to eliminate any free diclofenac sodium. The loaded diclofenac sodium was determined spectrophotometrically at 276 nm using UV-1800 spectrophotometer

(Shimadzu). The drug loading (%) and entrapment efficiency (%) were calculated using eqn (2) and (3):

$$\text{Drug loading } (\%) = \frac{\text{wt of drug in nanocomposite}}{\text{wt of nanocomposite}} \times 100 \quad (2)$$

$$\text{Drug entrapment efficiency } (\%) =$$
$$\frac{\text{weight of drug in nanocomposite}}{\text{weight of drug taken}} \times 100 \quad (3)$$

2.8.2 Transdermal delivery of diclofenac sodium. *In vitro* diclofenac sodium release was performed using a Diffusion Cell Apparatus (supplied by Orchid Scientific & Innovative India Pvt. Ltd., India) at pH 5.6 and temperature of 32 °C. Cellulose acetate dialysis membrane (LA390, average flat width – 25.27 mm, average diameter – 15.9 mm and capacity approximate – 1.99 mL cm^{-1}) was used as human skin replica[37] for delivery of diclofenac from the nanocomposite. The CMC–MWCNT nanocomposites were kept on the dialysis membrane which act as donor compartment. The entire release study was executed at a temperature of 32 ± 0.5 °C, as the human skin temperature is 32 °C.[37] The aliquots were withdrawn after regular time intervals and the volume was filled up with the same amount of fresh buffer. The diclofenac sodium release (%) was analysed spectrophotometrically at 276 nm. To investigate the release mechanism, Korsmeyer–Peppas model[42] was used (eqn (4))

$$\frac{M_t}{M_\infty} = Kt^n \quad (4)$$

where, M_t/M_∞, K, t and n signify the fraction of drug release at time t, the release constant, time and diffusion exponent, respectively.

2.8.3 Stability test of the drug in CMC and CMC–MWCNT 3 nanocomposites. The stability of diclofenac sodium in CMC and CMC–MWCNT nanocomposite was performed using humidity chamber. The drug loaded CMC and nanocomposite hydrogel were placed in the humidity chamber at a temperature of 40 ± 2 °C and relative humidity (RH) of 75 ± 5%.

3. Results and discussion

3.1 Preparation and characterization of composite

Nanocomposite derived from MWCNT and CMC was prepared by the ultrasonication of dispersed MWCNT into the carboxymethyl cellulose matrix. It is presumed that strong H-bonding as well as electrostatic interactions predominate between acid groups of MWCNT and hydroxyl/carboxyl groups of CMC as proposed in Scheme 1.

From the FTIR spectrum of CMC (Fig. 1a), it is obvious that the peak at 3423 cm^{-1} is owing to the stretching frequency of –OH groups. The peaks at 2917 and 1631 cm^{-1} are due to stretching vibrations of C–H and carboxylate groups, respectively. The peaks at 1428, 1333 and 1046 cm^{-1} are assigned to –CH$_2$ scissoring, –OH bending and C–O–C stretching respectively.[25–28] In the FTIR spectrum of CMC–MWCNT 3 nanocomposite (Fig. 1b), all the characteristics peaks of CMC are present. However, the –OH stretching vibration shifted to lower
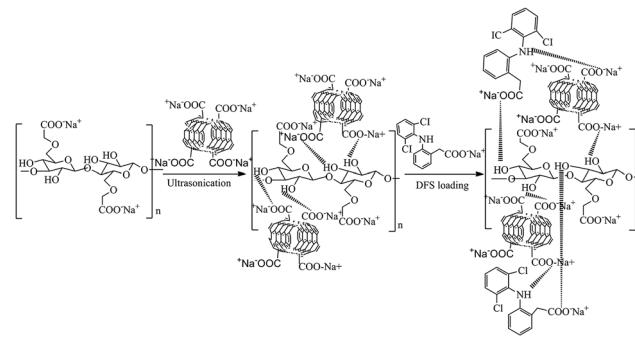
Scheme 1 Schematic representation for the preparation of nanocomposite and probable interaction between the drug and nanocomposite.

value (3318 cm^{-1}). Also the stretching vibration of COO$^-$ groups shifted to 1583 cm^{-1}. The shifting of peak values towards lower region in the composite indicates that H-bonding interaction prevails between CMC and carboxy functionalized nanotube as proposed in Scheme 1. Fig. 1c shows the FTIR spectrum of diclofenac sodium, which consist of the characteristic bands at 3384, 1580, 753 cm^{-1} corresponding to the NH stretching of secondary amine, –CO stretching of carboxyl ion and C–Cl stretching vibrations, respectively. Fig. 1d demonstrates the FTIR spectrum of drug loaded with CMC–MWCNT 3 nanocomposite, which clearly indicates that further shifting is obvious, indicating that H-bonding interactions are present between the composite and the drug as shown in Scheme 1.

Fig. S1, ESI† demonstrates the TGA and DTG profiles of CMC and CMC–MWCNT nanocomposite hydrogel. CMC has two distinct weight loss regions (Fig. S1a†). The first zone (weight loss: ~12%, temperature range: ~40–100 °C) corresponds to the presence of moisture and second weight loss region (weight
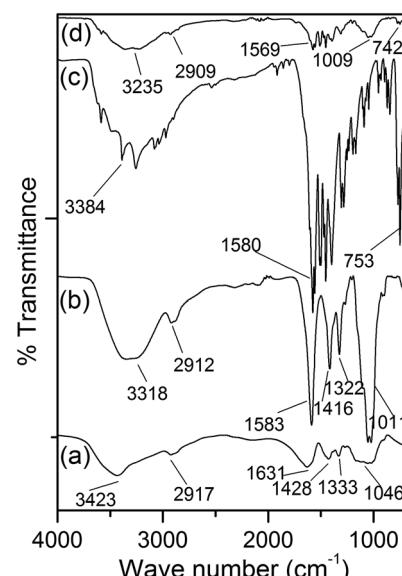
Fig. 1 FTIR spectra of (a) CMC, (b) CMC–MWCNT 3 (c) diclofenac sodium and (d) drug loaded nanocomposite.

loss: ~40%, temperature range: ~258–306 °C) is owing to the decarboxylation of CMC.[37] For CMC–MWCNT 3 nanocomposite (Fig. S1b†), one additional degradation zone has been observed (weight loss: ~10%, temperature range: ~450–700 °C), which is because of the degradation of MWCNT from the composite material. The delayed decomposition rate of CMC–MWCNT nanocomposite suggests the enhancement of thermal stability of the nanocomposite,[43] which is primarily because of the H-bonding as well as electrostatic interactions between MWCNT and CMC in the nanocomposite. Moreover, we have also calculated the amount of filler retained in the nanocomposite, which was found to be ~1.5%.

FESEM analyses suggests that CMC (Fig. S2, ESI†) has rough fibrillar morphology. After modification, the surface morphology of CMC–MWCNT 3 nanocomposite (Fig. 2a) significantly changed to relatively smooth and co-continuous where distribution of MWCNT (indicated by blue arrow) has been clearly visualized (Fig. 2a). This morphology probably be suitable for more amount of drug encapsulation on the composite surface.

The 2- and 3-dimensional AFM phase images of CMC–MWCNT 3 nanocomposite are shown in Fig. 2b and c. In the phase images of nanocomposite (Fig. 2b and c), two distinct colours signify two different types of materials are present in the nanocomposite. The deep colour is due to the presence of CMC moiety, while white colour is responsible for the existence of carbon nanotube. Besides, the phase images also suggest the fine dispersion of nanotubes in the nanocomposite with a good compatibility between CMC and MWCNT.

Incorporation of MWCNT not only affects the composition of hydrogel, but also changed its surface morphology. The TEM image of CMC–MWCNT 3 nanocomposite (Fig. 2d) reveals that MWCNT has a random orientation in the composite material. The single MWCNT appears as nano-scale fibril shaped with

diameter less than 100 nm and the length of a single fibril is about several hundred of nano meters. The micrograph also depict that the MWCNT nanofibril is regularly dispersed in the composite without agglomeration and formed a homogeneous composition.[44]

3.2 Rheological characteristics

From Fig. S3, ESI,† it is apparent that for CMC and all the nanocomposite hydrogels, shear viscosity declined with rise in shear rate, indicating the shear thinning non-Newtonian behaviour. In addition, the increase in shear viscosity in case of composite materials suggests the better interactions between the organic polymer and inorganic nanofiller. At lower concentration, uniform filler dispersion ensures better interactions, ensuing higher shear viscosity (CMC–MWCNT 3).

Fig. 3a and b demonstrate that elastic modulus (G') of CMC and CMC–MWCNT 3 is greater than that of viscous modulus (G''), which imply the elastic nature of gel state. Moreover, the increase of G' and G'' values with the increase of frequency indicates the increase in elastic nature of the CMC and CMC–MWCNT nanocomposite. However, the wide separation of G' and G'' in case of nanocomposite hydrogel compared to CMC is mainly because of the hetero phase interactions (i.e. between CMC and MWCNT, as proposed in Scheme 1), which is completely absent in CMC. Additionally the higher value of (G'/G'') of CMC–MWCNT 3 nanocomposite compared to CMC (Fig. 3b) signifies that the gel strength of the nanocomposite increased considerably owing to incorporation of MWCNT. It is also obvious that after certain shear stress, both G' and G'' decreased sharply, which is an indication of breakdown of the gel network.[25]

3.3 Swelling properties

Fig. S4, ESI† demonstrates the swelling characteristics of CMC and various nanocomposites. It is obvious (Table 1 and Fig. S4, ESI†) that the % swelling of CMC is higher, while the rate parameter is lower in comparison to CMC–MWCNT
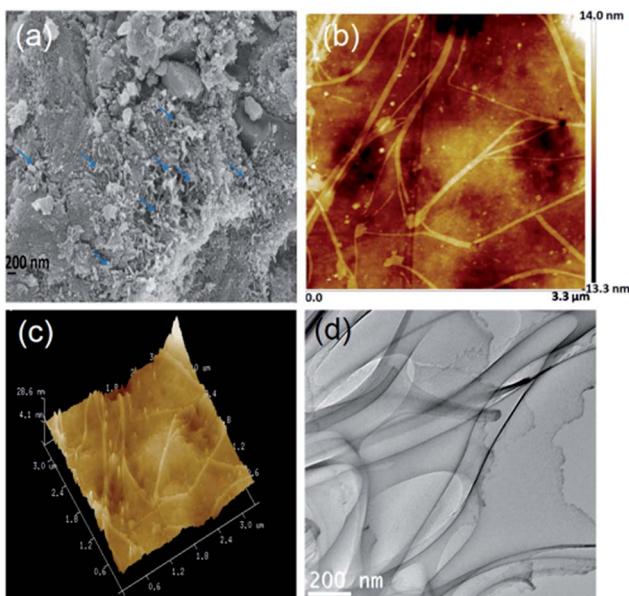

Fig. 2 (a) FESEM, (b) 2D topographic, (c) 3-D topographic and (d) TEM images of CMC–MWCNT 3 nanocomposite.
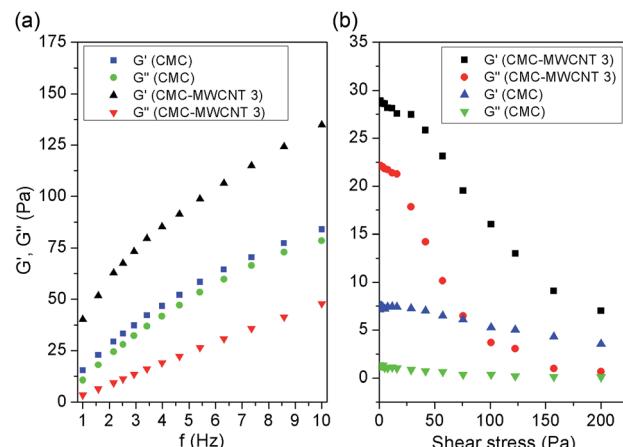

Fig. 3 Plots between (a) G' and G'' vs. frequency, (b) G' and G'' vs. shear stress of CMC and CMC–MWCNT 3 nanocomposite.

Table 1 Reaction parameters of various nanocomposites, equilibrium swelling ratio and values of swelling kinetics and drug release parameters (for each synthesis, 0.5 g CMC was taken)

Polymer/nanocomposite	MWCNT (g)	% ESR	Value of rate parameter (τ)	Diffusion exponent (n)	Yield stress σ_y	G'/G''
CMC	0.00	4280 ± 212	129.87 ± 2.34	0.47	29.75	1.51
CMC–MWCNT 1	0.00125	3525 ± 175	138.88 ± 1.60	0.48	29.27	4.62
CMC–MWCNT 2	0.00250	3382 ± 168	140.45 ± 3.62	0.51	42.89	10.25
CMC–MWCNT 3	0.0050	2221 ± 109	165.56 ± 1.98	0.63	70.45	6.85
CMC–MWCNT 4	0.0075	2835 ± 140	147.06 ± 2.99	0.58	52.47	10.47

nanocomposites. This is because, the hydrophilic groups (–OH and –COOH) present in CMC moiety strongly bound with large number of water molecules by H-bonding, which increased the % swelling of CMC. On the other hand, because of physical interactions (as explained earlier) between CMC and MWCNT in the nanocomposite network, less number of water molecules can enter into the composite material, resulting lower % swelling than that of CMC.

3.4 Biodegradation results

Fig. S5, ESI† depicts the biodegradation result of CMC–MWCNT 3 nanocomposite film for 0, 3, 7 and 14 days. It is obvious that the mass of the nanocomposite hydrogel decreased progressively in presence of lysozyme. Lysozyme degrades the polysaccharides by the hydrolysis of the glycosidic bonds of the hexameric sugar ring. The progressive mass loss indicates the biodegradable nature of the CMC–MWCNT composite.

3.5 Biocompatibility analysis

The cells grown in both control media and CMC–MWCNT 3 nanocomposite treated media maintained sustainable population of RFBs throughout the study period (Fig. 4). Assessment of cellular viability (1, 3 and 7 days), by measuring metabolic activity of cells grown in normal media and media supplemented with nanocomposite (1 mg mL^{-1}) indicated that cells grown in media supplemented with nanocomposite proliferated at a higher rate than that of cells grown in normal media (Fig. 4b). At 7 days, the number of cells grown in

nanocomposite medium and normal medium was 4.33×10^4 and 3.21×10^4, respectively.

The higher number of cell population on the CMC–MWCNT 3 nanocomposite medium may be because of the enhanced metabolic activity of the cells. The results confirmed the cytocompatible and non-toxic nature of the CMC–MWCNT nanocomposite.

On day 7, rhodamine–phalloidin and DAPI staining of the cells grown in media supplemented with CMC–MWCNT 3 nanocomposite revealed prominent feature of each nucleus, well surrounded by clearly demarcated F-actin filaments, an indication that a layer of cells is spreading on the surface (Fig. 4c and d). As F-actin signifies the existence of thin filaments in cells and allow the cells to interact with surroundings, the fluorescent images clearly establish that cells grown in CMC–MWCNT 3 nanocomposite treated medium are promoting favourable environment (Fig. 4d) for cell–cell interactions, similar to the cells grown in normal medium (Fig. 4c).

4. Transdermal delivery of diclofenac sodium

Diclofenac sodium has –COO$^-$ groups, while both CMC and CMC–MWCNT 3 have –OH and –COOH groups. The drug molecules interact CMC and nanocomposites through H-bonding interactions (as demonstrated in Scheme 1). Fig. S6, ESI† demonstrates the absorbance values of 0.8 mg mL^{-1} diclofenac sodium solution and supernatant of various nanocomposites after 4 h. Because of the presence of MWCNT as well as lower % swelling, CMC–MWCNT 3 nanocomposite has higher loading (15.05%) and encapsulation efficiency (90.31%) rather than CMC and other nanocomposites (Fig. S6 and Table S1, ESI†). The loading duration of the optimized nanocomposite was varied from 15 min to 4 h and it was observed that % loading and % entrapment efficiency of the nanocomposite was maximum at 4 h (Table S1, ESI†).

The % cumulative release of diclofenac sodium from CMC and CMC–MWCNT nanocomposites are shown in Fig. 5a. For nanocomposite hydrogels, drug release depends on the % swelling, nanoparticle density and gel strength of that material. As the drug release is fully controlled by the diffusion process, rate of swelling is the key factor for release of drug. From the release profiles (Fig. 5a), it is obvious that CMC released diclofenac sodium in much faster rate compared to the composites. This is because of higher rate of swelling and lower gel strength
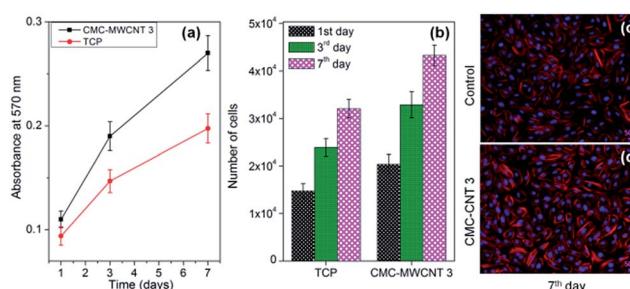

Fig. 4 (a) Cell viability result, (b) cell proliferation result of control and CMC–MWCNT 3 nanocomposite study by MTT assay (SD ± 3), and (c), (d) cellular attachment of RFBs by rhodamine–phalloidin and DAPI assay at different time periods.
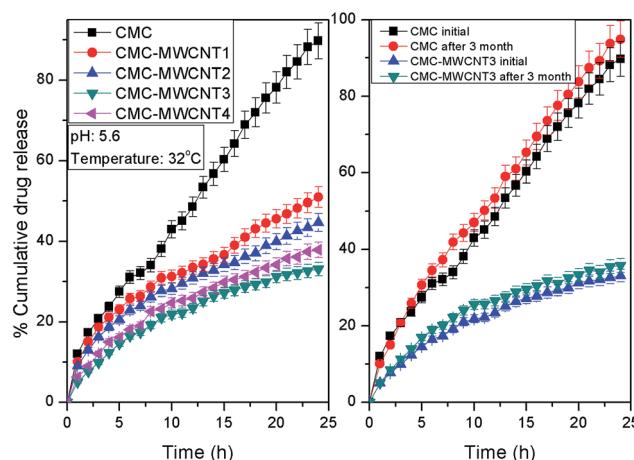
Fig. 5 Diclofenac release from (a) CMC and various nanocomposites and (b) stability study of drug loaded CMC and CMC–MWCNT 3 nanocomposite for 3 months.

of CMC. On the other hand, among the nanocomposites, CMC–MWCNT 3 demonstrates most sustained release behaviour. This is mainly due to the better matrix–filler interaction at this composition, lower equilibrium swelling as well as maximum gel strength than that of other nanocomposites (Table 1). Besides, the release of diclofenac sodium from the nanocomposite hydrogel followed non-Fickian diffusion mechanism (Table 1).

4.1 Stability test results

Stability of the diclofenac sodium loaded with CMC and CMC–MWCNT 3 were studied (Fig. 5b and Table S2, ESI†) to investigate the effect of environmental factors on the drug release for 3 months.[45] It is obvious that ~98% drug remained stable after 3 months in the composite formulation at 40 °C/75% RH, while the drug's stability is poor using CMC as drug carrier.

5.   Conclusion

From above experimental observations, it is obvious that a biodegradable and non-cytotoxic hybrid nanocomposite hydrogel has been developed from CMC and MWCNT by ultrasonication. Various chemical characterizations confirmed the formation of the CMC–MWCNT nanocomposite. Cell proliferation study implies that the hybrid nanocomposite is biocompatible towards rat fibroblasts (RFBs). Biodegradation study using lysozyme chloride confirmed the biodegradable nature of the composite. Rheological experiments suggest that composite demonstrates better gelling characteristics in compared to neat CMC. The transdermal release study revealed that CMC–MWCNT nanocomposite released the diclofenac sodium in a controlled way and may be an excellent alternative as transdermal device for diclofenac sodium. Finally, the stability study predicts that the drug remains stable upto 3 months in presence of composite matrix.

References

1 A. C. Albertsson, J. Voepel, U. Edlund, D. Olof and M. S. Lindblad, *Biomacromolecules*, 2010, **11**, 1406–1411.

2 M. Vargas, J. Weiss and D. J. McClements, *Langmuir*, 2007, **23**, 13059–13065.

3 L. Cao, B. Cao, C. Lu, G. Wang and L. Y. J. Ding, *J. Mater. Chem. B*, 2015, **3**, 1268–1280.

4 B. Balakrishnan and R. Banerjee, *Chem. Rev.*, 2011, **111**, 4453–4474.

5 J. Yu, W. Ha, J. Sun and Y. Shi, *ACS Appl. Mater. Interfaces*, 2014, **6**, 19544–19551.

6 D. Das, R. Das, P. Ghosh, S. Dhara, A. B. Panda and S. Pal, *RSC Adv.*, 2013, **3**, 25340–25350.

7 B. Bhowmick, G. Sarkar, D. Rana, I. Roy, N. R. Saha, S. Ghosh, M. Bhowmik and D. Chattopadhyay, *RSC Adv.*, 2015, **5**, 60386–60391.

8 Q. Chen, H. Chen, L. Zhu and J. Zheng, *J. Mater. Chem. B*, 2015, **3**, 3654–3676.

9 S. G. Roy, U. Haldar and P. De, *ACS Appl. Mater. Interfaces*, 2014, **6**, 4233–4241.

10 T. Bhunia, A. Giri, T. Nasim, D. Chattopadhyay and A. Bandyopadhyay, *Carbon*, 2013, **52**, 305–315.

11 G. Trakakis, G. Anagnostopoulos, L. Sygellou, A. Bakolas, J. Parthenios and D. Tasis, *Chem. Eng. J.*, 2015, **281**, 793–803.

12 M. Aykol, B. Hou, R. Dhall, S. W. Chang, W. Branham and J. Qiu, *Nano Lett.*, 2014, **14**, 2426–2430.

13 R. Sridhar, R. Lakshminarayanan, K. Madhaiyan, V. A. Barathi, K. H. C. Limh and S. Ramakrishna, *Chem. Soc. Rev.*, 2015, **44**, 790–814.

14 E. A. Appel, M. W. Tibbitt, J. M. Greer, O. S. Fenton, K. Kreuels and D. G. Anderson, *ACS Macro Lett.*, 2015, **4**, 848–852.

15 H. D. Huang, C. Y. Liu, L. Q. Zhang, G. J. Zhong and Z. M. Li, *ACS Sustainable Chem. Eng.*, 2015, **3**, 317–324.

16 S. Ghorai, A. Sinhamahpatra, A. Sarkar, A. B. Panda and S. Pal, *Bioresour. Technol.*, 2012, **119**, 181–190.

17 S. Merino, C. Martín, K. Kostarelos, M. Prato and E. Vázquez, *ACS Nano*, 2015, **9**, 4686–4697.

18 R. Das, D. Das, P. Ghosh, S. Dhara, A. B. Panda and S. Pal, *RSC Adv.*, 2015, **5**, 27481–27490.

19 A. K. Sarkar, A. Saha, A. B. Panda and S. Pal, *Chem. Commun.*, 2015, **51**, 16057–16060.

20 J. S. Im, B. C. Bai and Y. S. Lee, *Biomaterials*, 2010, **31**, 1414–1419.

21 A. Giri, T. Bhunia, S. R. Mishra, L. Goswami, A. B. Panda and A. Bandyopadhyay, *RSC Adv.*, 2014, **4**, 13546–13556.

22 A. M. Wokovich, S. Prodduturi, W. H. Doub, A. S. Hussain and L. F. Buhse, *Eur. J. Pharm. Biopharm.*, 2006, **64**, 1–8.

23 Q. Fan, K. K. Sirkar and B. Michniak, *J. Membr. Sci.*, 2008, **321**, 240–248.

24 J. R. Walter and S. Xu, *Drug Discovery Today*, 2015, **20**, 1293–1299.

25 K. Bekkour, D. S. Waterhouse and S. S. Wadhwa, *Food Res. Int.*, 2014, **66**, 247–256.

26 D. R. Biswal and R. P. Singh, *Carbohydr. Polym.*, 2004, **57**, 379–387.

27 M. Hashem, S. Sharaf, M. M. Abd El-Hady and A. Hebeish, *Carbohydr. Polym.*, 2013, **92**, 407–413.

28 J. S. Bridel, T. Azaïs, M. Morcrette, J. M. Tarascon and D. Larcher, *Chem. Mater.*, 2010, **22**, 1229–1241.

29 U. S. Vogl, P. K. Das, A. Z. Weber, M. Winter, R. Kostecki and S. F. Lux, *Langmuir*, 2014, **30**, 10299–10307.

30 H. Peng, G. Ma, W. Ying, A. Wang, H. Huang and Z. Lei, *J. Power Sources*, 2012, **211**, 40–45.

31 Y. Chenga, B. Fengb, X. Yanga, P. Yanga, Y. Dinga and Y. Chena, *Sens. Actuators, B*, 2013, **182**, 288–293.

32 N. Hintshoa, L. Petrika, A. Nechaeva, S. Titinchia and P. Ndungub, *Appl. Catal., B*, 2014, **156–157**, 273–283.

33 J. Y. Ahn, J. H. Kim, J. M. Kim, D. Lee and S. H. Kim, *Sol. Energy*, 2014, **107**, 660–667.

34 A. N. Golikand, M. Asgari and E. Lohrasbi, *Int. J. Hydrogen Energy*, 2011, **36**, 13317–13324.

35 G. Sanzó, C. Tortolini, R. Antiochia, G. Favero and F. Mazzei, *J. Nanosci. Nanotechnol.*, 2015, **15**, 3423–3428.

36 E. Axpe, L. Bugnicourt, D. Merida, M. G. Goikoetxea, I. Unzueta and R. S. Eugenia, *J. Mater. Chem. B*, 2015, **3**, 3169–3176.

37 A. Giri, M. Bhowmick, S. Pal and A. Bandyopadhyaya, *Int. J. Biol. Macromol.*, 2011, **49**, 885–893.

38 R. Kasperek, E. Zimmer, W. Jawie and E. Poleszak, *Acta Pol. Pharm.*, 2015, **72**, 527–538.

39 V. Ranaa, P. Raia, A. K. Tiwarya, R. S. Singh, J. F. Kennedy and C. J. Knill, *Carbohydr. Polym.*, 2011, **83**, 1031–1047.

40 T. Freier, H. S. Koh, K. Kazazian and M. S. Shoichet, *Biomaterials*, 2005, **26**, 5872–5878.

41 R. Justin and B. Chen, *Carbohydr. Polym.*, 2014, **103**, 70–80.

42 R. W. Korsmeyer, R. Gurny, E. Doelker, P. Buri and N. A. Peppas, *Int. J. Pharm.*, 1983, **15**, 25–35.

43 B. Sivakumar, R. G. Aswathy, Y. Nagaoka, M. Suzuki, T. Fukuda and Y. Yoshida, *Langmuir*, 2013, **29**, 3453–3466.

44 W. Wanga and A. Wanga, *Carbohydr. Polym.*, 2010, **82**, 83–91.

45 D. Das, P. Ghosh, S. Dhara, A. B. Panda and S. Pal, *ACS Appl. Mater. Interfaces*, 2015, **7**, 4791–4803.